ISSN 2616-5767 Vol.8, Issue 3: 41-50, DOI: 10.25236/AJETS.2025.080307

Ride Quality Improvement Based on the H∞ Loop Shaping Control Method for Semi-Active Suspension System of High Speed Train

Luping Yang[1,a,*]

[1]*Mechanical and Electrical Institute, Chengdu Product Quality Supervision and Inspection Institute, Chengdu, China*
[a]*1529760825@qq.com*
**Corresponding author*

Abstract: *This paper focuses on the ride quality and operation stability of high-speed train by employing the lateral semi-active secondary suspension, First, the full-scale railway vehicle dynamics with 17-degree-of-free (DOF) are introduced, where German low disturbance and high disturbance track irregularities are considered. Then, in order to improve the operation stability and robust stability of the train system at the same time, the $H\infty$ loop shaping controler is proposed. This controller has good results in dealing with the structural uncertainty of the system, and the coprime factorization decomposition uncertainty modeling used is more general and universal than other uncertainty modeling. Moreover, the train simulation model of CRH3 is established in SIMPACK. Finally, the German low and high disturbance track irregularities are employed to show the efficiency of the proposed loop-shaping-control-based semi-active suspension by comparing with the open loop.*

Keywords: *High Speed Train; Semi-Active Suspension; H-Infinity Loop Shaping Control; Operation Stability*

1. Introduction

As a proficient and cost-effective type of transportation, the high-speed train has received a lot of attentions in the past few decades, especially in China. However, with the continuous improvement of train speed and the application of lightweight design, the vibration caused by track irregularities, cross winds, tunnels, bridges and other factors has a significant impact on the running stability, ride confort and safety of high-speed train. Hence, the active suspension system [1-3] or semi-active suspension system [4-10] is applied to suppress car body vibration by adopting modern control methods.

Semi-active suspension system has been widely used in theoretical research and practical application of train due to its excellent vibration isolation performance, low external energy consumption, simple structure and strong robustness. In order to further improve the ride quality, more and more advanced control strategies are being explored and applied.

In the devoted literatures, semi-active control strategies can usually be divided into four parts. The first one is sky-hook damping control method. This method was first proposed by Professor Karnopp from the University of California [1]. In order to reduce the derailment coefficient of railway vehicle, a new semi-active control strategy based on the skyhook control theory was presented [11]. The second one is linear quadratic (LQ) optimal control method. To improve the ride quality of train, an linear quadratic Gaussian (LQG) controller with a Kalman estimator was presented to estimate acceleration state variables in [12-13]. To improve ride confort and hunting stability simultaneous, a LQG control strategy was employed to secondary and primary suspension [14]. The third strategy is $H\infty$ robust control.For reducing lateral vibration acceleration of carbody with a semi-active suspension system, a H∞ controller was adopted [15]. In order to improve the lateral ride quality,semi-active H∞ control with magnetorheological (MR) dampers for railway vehicle suspension systems is investigated [16]. The last one is Intelligent control strategy, such as adaptive control, fuzzy control, neural network control, genetic algorithm, etc. In [17],the low-cost adaptive fault-tolerant PD controller was developed to suppresses excessive motion of train body in vertical and lateral directions effectively. In [18], the fuzzy logic and PID controllers were employed for the active vertical suspension system. A fuzzy control strategy based on particle swarm optimization was proposed for the lateral semi-active suspension [19].

ISSN 2616-5767 Vol.8, Issue 3: 41-50, DOI: 10.25236/AJETS.2025.080307

In this paper, the $H\infty$ loop shaping control method is proposed to improve the train's ride quality. For the lateral vibration suppression of trains, $H\infty$ controller can achieve good results, but the effect of this method in dealing with the structural uncertainty is not ideal. $H\infty$ Loop shaping method has been widely used in the field of modern control. At present, loop shaping method has been applied in the design of various aircraft control algorithms in aerospace [20-21], robot[22], vehicle control and vibrarion control[23]. Therefore, a $H\infty$ loop shaping control method is proposed in this paper to design the damping controller for the second suspension system. The purpose of this paper is to suppress the lateral acceleration of train body by using $H\infty$ loop shaping control algorithm, and improve ride comfort and guarantee operation stability.

2. Analysis Model Of Railway Vehicle

2.1 Dynamics of Railway Vehicle

The railway vehicle consists of a car body, two bogies and four wheelsets,as conceptually shown in Figure. 1. The two bogies, which are identified as the front and rear bogies, are connected to the car body by the secondary suspension. Each of the two bogies is also connected to two wheelsets by the primary suspension. The motions of the car body, the bogies, and the wheelsets of the railway vehicle, the control forces of actuators, and the disturbances generated by track irregularities involved in the modeling are listed in Table 1, where $i=1,2,\ j=1,2,3,4$.

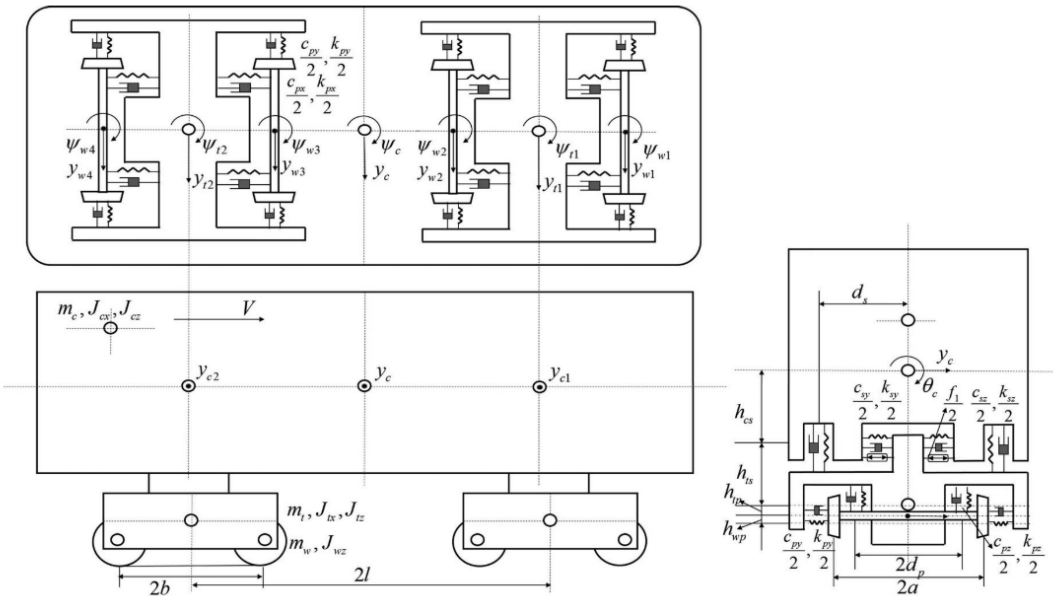

Figure 1: Analytical model of a full-scale railway vehicle integrated with actuators

Table 1: 17-DOF,Control force ,and Disturbance of the lateral active secondary suspension system.

Symbol		Definition
17-DOF	y_c, y_{ti}	Lateral displacement of car body or bogie.
	y_{wj}	Lateral displacement of wheelset.
	φ_c, φ_{ti}	Lateral displacement of wheelset.
	φ_{wj}	Yaw angle of wheelset.
	θ_c, θ_{ti}	Roll angle of car body or bogies
Control force	u_i	Front or rear active force produced by the actuators equipped on front or rear bogie.
Disturbance	y_{aj}	Lateral alignment of track irregularities related to the four wheelset.
	θ_{clj}	Cross-level of track irregularities related to the four wheelset.

Considering the configuration of spring and damping of high speed train suspension system, the following typical train dynamics for the car body, bogies, and wheelsets are established by using

ISSN 2616-5767 Vol.8, Issue 3: 41-50, DOI: 10.25236/AJETS.2025.080307

Newton's law.

1) Car body dynamics:

$$m_c\ddot{y}_c = -k_{sy}(2y_c - 2h_{cs}\theta_c - y_{t1} - y_{t2} - h_{ts}\theta_{t1} - h_{ts}\theta_{t2}) - c_{sy}(2\dot{y}_c - 2h_{cs}\dot{\theta}_c - \dot{y}_{t1} - \dot{y}_{t2} - h_{ts}\dot{\theta}_{t1} - h_{ts}\dot{\theta}_{t2}) + u_1 + u_2 \tag{1}$$

$$I_{cz}\ddot{\psi}_c = -k_{sx}(2\psi_c - \psi_{t1} - \psi_{t2})d_s^2 - -c_{sx}(2\dot{\psi}_c - \dot{\psi}_{t1} - \dot{\psi}_{t2})d_s^2 - k_{sy}(2l\psi_c - y_{t1} + y_{t2} - h_{ts}\theta_{t1} + h_{ts}\theta_{t2})l - c_{sy}(2l\dot{\psi}_c - \dot{y}_{t1} + \dot{y}_{t2} - h_{ts}\dot{\theta}_{t1} + h_{ts}\dot{\theta}_{t2})l + (u_1 - u_2)l \tag{2}$$

$$I_{cx}\ddot{\theta}_c = k_{sy}(2y_c - 2h_{cs}\theta_c - y_{t1} - y_{t2} - h_{ts}\theta_{t1} - h_{ts}\theta_{t2})h_{cs} + c_{sy}(2\dot{y}_c - 2h_{cs}\dot{\theta}_c - \dot{y}_{t1} - \dot{y}_{t2} - h_{ts}\dot{\theta}_{t1} - h_{ts}\dot{\theta}_{t2})h_{cs} - k_{sz}(2\theta_c - \theta_{t1} - \theta_{t2})d_s^2 - c_{sz}(2\dot{\theta}_c - \dot{\theta}_{t1} - \dot{\theta}_{t2})d_s^2 - (u_1 + u_2)h_{cs} \tag{3}$$

2) Bogie dynamics($i = 1,2$):

$$m_t\ddot{y}_{ti} = k_{sy}(y_c - (-1)^i l\psi_c - h_{cs}\theta_c - y_{ti} - h_{ts}\theta_{ti}) + c_{sy}(\dot{y}_c - (-1)^i l\dot{\psi}_c - h_{cs}\dot{\theta}_c - \dot{y}_{ti} - h_{ts}\dot{\theta}_{ti}) - k_{py}(2y_{ti} - 2h_{tp}\theta_{ti} - y_{w(2i-1)} - y_{w(2i)}) - c_{py}(2\dot{y}_{ti} - 2h_{tp}\dot{\theta}_{ti} - \dot{y}_{w(2i-1)} - \dot{y}_{w(2i)}) - u_i \tag{4}$$

$$I_{tz}\ddot{\psi}_{ti} = k_{sx}(\psi_c - \psi_{ti})d_s^2 + c_{sx}(\dot{\psi}_c - \dot{\psi}_{ti})d_s^2 - k_{px}(2\psi_{ti} - \psi_{w(2i-1)} - \psi_{w(2i)})d_p^2 - c_{px}(2\dot{\psi}_{ti} - \dot{\psi}_{w(2i-1)} - \dot{\psi}_{w(2i)})d_p^2 - k_{py}b(2b\psi_{ti} - y_{w(2i-1)} + y_{w(2i)}) - c_{py}b(2b\dot{\psi}_{ti} - \dot{y}_{w(2i-1)} + \dot{y}_{w(2i)}) \tag{5}$$

$$I_{tx}\ddot{\theta}_{ti} = k_{sy}h_{ts}(y_c - (-1)^i l\psi_c - h_{cs}\theta_c - y_{ti} - h_{ts}\theta_{ti}) + c_{sy}h_{ts}(\dot{y}_c - (-1)^i l\dot{\psi}_c - h_{cs}\dot{\theta}_c - \dot{y}_{ti} - h_{ts}\dot{\theta}_{ti}) + k_{sz}(\theta_c - \theta_{ti})d_s^2 + c_{sz}(\dot{\theta}_c - \dot{\theta}_{ti})d_s^2 + k_{py}h_{tp}(2y_{ti} - 2h_{tp}\theta_{ti} - y_{w(2i-1)} - y_{w(2i)}) + c_{py}h_{tp}(2\dot{y}_{ti} - 2h_{tp}\dot{\theta}_{ti} - \dot{y}_{w(2i-1)} - \dot{y}_{w(2i)}) - 2k_{pz}d_p^2\theta_{ti} - 2c_{pz}d_p^2\dot{\theta}_{ti} - f_i h_{ts} \tag{6}$$

3) Wheelset dynamics($i = 1,2$, while $j = 1$, $i = 3,4$, while $j = 2$);

$$m_w\ddot{y}_{wi} = k_{py}(y_{tj} - (-1)^i a\psi_{tj} - h_{tp}\theta_{tj} - y_{wi}) + c_{py}(\dot{y}_{tj} - (-1)^i a\dot{\psi}_{tj} - h_{tp}\dot{\theta}_{tj} - \dot{y}_{wi}) - 2f_{22}\left[\frac{1}{V}(1 + \frac{\sigma r_0}{Vb})\dot{y}_{wi} - \frac{\sigma r_0}{Vb}\dot{y}_{ai} - \frac{\sigma r_0^2}{Vb}\theta_{cli} - \psi_{wi}\right] - k_{gy}(y_{wi} - y_{ai} - r_0\theta_{cli}) \tag{7}$$

$$I_{wz}\ddot{\psi}_{wi} = k_{px}(\psi_{tj} - \psi_{wi})d_p^2 + c_{px}(\dot{\psi}_{tj} - \dot{\psi}_{wi})d_p^2 - 2f_{11}\left[\frac{\lambda_e b}{r_0}(y_{wi} - y_{ai} - r_0\theta_{cli}) + \frac{b^2}{V}\dot{\psi}_{wi}\right] + k_{g\psi}\psi_{wi} \tag{8}$$

2.2 State-space Formulation

Let $w_1 = [y_{a1}, y_{a2}, y_{a3}, y_{a4}, \theta_{cl1}, \theta_{cl2}, \theta_{cl3}, \theta_{cl4}]$ $q = [y_c, \psi_c, \theta_c, y_{t1}, \psi_{t1}, \theta_{t1}, y_{t2}, \psi_{t2}, \theta_{t2}, y_{w1}, \psi_{w1}, y_{w2}, \psi_{w2}, y_{w3}, \psi_{w3}, y_{w4}, \psi_{w4}]^T$, $w = [w_1, \dot{w}_1]^T$ and $u = [u_1, u_2]^T$. Then,the above equations (1)-(8) can be rewritten in the following matrix form:

$$M\ddot{q} + C\dot{q} + Kq = E_u u + E_w w \tag{9}$$

Where $M \in R^{17\times17}$ is the mass coefficient matrix of the train system; $C \in R^{17\times17}$ is the damping coefficient matrix; $K \in R^{17\times17}$ is the stiffness coefficient matrix; $E_u \in R^{17\times2}$, $E_w \in R^{17\times16}$ are the controlled force and disturbance matrixes,respectively.

According to the standards of railway vehicle,we have that $\ddot{y}_c$ is used to evaluate the ride quality. Consider placing the acceleration sensor on the train body above the front and rear bogie. Based on the following relationship: $y_c = (y_{c1} + y_{c2})/2; \psi_c = (y_{c1} - y_{c2})/2l$. Where y_{c1}, y_{c2} represent the lateral displacement of the car body above the front and rear bogies,respectively. It can be known that lateral acceleration and yaw acceleration of car body meet the following equation: $\ddot{y}_c = (\ddot{y}_{c1} + \ddot{y}_{c2})/2; \ddot{\psi}_c = (\ddot{y}_{c1} - \ddot{y}_{c2})/2l$. Let the state variable of the system be expressed as: $x = [q \quad \dot{q}]^T$. For the purpose of suppressing lateral vibration of vehicle body, it is assumed that the controlled output variables of the train system are denoted as follows: $y = [\ddot{y}_{c1} \quad \ddot{y}_{c2}]^T$. Thus,the state-space equations can be written as follows:

$$\begin{cases} \dot{x} = Ax + B_1 w + B_2 u \\ y = Cx + D_1 w + D_2 u \end{cases} \tag{10}$$

Where $A \in R^{34\times34}$, $B_1 \in R^{34\times16}$, $B_2 \in R^{34\times2}$, $C \in R^{2\times34}$, $D_1 \in R^{2\times16}$, $D_2 \in R^{2\times2}$ are the system matrices derived from dynamic equations (1)-(8).

ISSN 2616-5767 Vol.8, Issue 3: 41-50, DOI: 10.25236/AJETS.2025.080307

2.3 Track irregularities

The lateral vibration of the train is mainly caused by the lateral alignment(y_{ai}) and cross level(θ_{cli}) of the track irregularities. Thus, these two irregularity signals are used as external excitation sources.

During the operation of the train, due to the reason of wheelset contact distance and truck center pin spacing, the lateral alignment irregularity and cross level irregularity meet the following requirements, where $i=1,2,3,4$, τ_1=2a/V , τ_2=2l/V , τ_3=$2(a+l)/V$,and V denotes running velocity. Let $\hat{W}_w(s)=\begin{bmatrix}1 & e^{-\tau_1 s} & e^{-\tau_2 s} & e^{-\tau_3 s}\end{bmatrix}^T$. Then, we can get : $d(s)=W_w(s)w(s)$. Where $W_w(s)=diag\left\{\hat{W}_w,\hat{W}_w,\hat{W}_w,\hat{W}_w\right\}$.

$$\begin{aligned} &y_{a2}(t)=y_{a1}(t-\tau_1), y_{a3}(t)=y_{a1}(t-\tau_2)\\ &y_{a4}(t)=y_{a1}(t-\tau_3), \theta_{cl2}(t)=\theta_{cl1}(t-\tau_1)\\ &\theta_{cl3}(t)=\theta_{cl2}(t-\tau_2),\quad \theta_{cl4}(t)=\theta_{cl3}(t-\tau_3) \end{aligned} \tag{11}$$

The lateral alignment and cross level track irregularities of German track spectrum are usually described by their power spectral densitm ies (PSDs), which are denoted as:

$$S_a(\Omega)=\frac{A_a\Omega_c^2}{(\Omega^2+\Omega_r^2)(\Omega^2+\Omega_c^2)};S_c(\Omega)=\frac{A_v b^{-2}\Omega_c^2\Omega^2}{(\Omega^2+\Omega_r^2)(\Omega^2+\Omega_c^2)(\Omega^2+\Omega_s^2)} \tag{12}$$

Where Ω represents spatial frequency; Ω_c、Ω_s and Ω_r all denotes runcated wavenumbers (rad/m); A_a and A_v are the scalar factors used to denote the amplitude of track irregularities ($m^2\cdot m/rad$). The value of these scalar factors are listed in Table 2.

Table 2: The parameters of german track irregularities.

	Ω_c	Ω_r	Ω_r	A_a	A_v
Low disturbance	0.8246	0.0206	0.4380	2.119×10^{-7}	6.125×10^{-7}
High disturbance	0.8246	0.0206	0.4380	4.032×10^{-7}	1.08×10^{-6}

3. $H\infty$ Loop Shaping Controlfor High-Speed Train

3.1 Loop shaping

The left coprime factorization of the train system G is described as follows $G=\tilde{M}^{-1}\tilde{N}$. The left coprime factor perturbed plant denoted as: $G_\Delta(s)=(\tilde{M}+\Delta_M)^{-1}(\tilde{N}+\Delta_N)$. Where $(\tilde{M},\tilde{N})$ are assumed to be a left coprime factorization ,and $\tilde{M},\tilde{N}\in RH_\infty;\Delta_M,\Delta_N$ is the stable and unknown perturbation, and satisfies $\left\|\Delta_M \quad \Delta_N\right\|_\infty<\varepsilon$, in which ε denotes the system stability margin. In order to cope with environmental variability and unknown factors during the train operation, the stability margin is required to satisfy $\varepsilon>0.3$.

According to the superposition principle of linear system, the train system output can be expressed as: $y=G_u(s)u(s)+G_w(s)d(s)$. Where $G_u(s)=C(sI-A)^{-1}B_2+D_2$, represents the transfer function from the controlled input to the system output; $G_w(s)=C(sI-A)^{-1}B_1+D_1$, represent the transfer function from track irregularity disturbance to system output.

Under the influence of input disturbance and interference noise, the close-loop output of the train system can be obtained as follows:

$$Y(s)=(1+G_u(s)K(s))^{-1}G_w(s)D(s)-(1+G_u(s)K(s))^{-1}G_u(s)K(s)N(s)=S_uG_w(s)D(s)-T_uN(s) \tag{13}$$

Where $D(s)$ is disturbance of track irregularity; $N(s)$ is the output noise of the system; $S_u=(1+G_u(s)K(s))^{-1}$ and $T_u=(1+G_u(s)K(s))^{-1}G_u(s)K(s)$ denote the sensitivity function and the supplementary sensitivity function of the train system,respectively. It is not difficult to see that $G_w(s)D(s)$ denotes the open loop transfer function of the system. Let's assume $G_w(s)D(s)$ as an external disturbance, then Equation (13) can be rewritten as:

ISSN 2616-5767 Vol.8, Issue 3: 41-50, DOI: 10.25236/AJETS.2025.080307

$$Y(s) = S_u W(s) - T_u N(s) \tag{14}$$

In order to make the system output as small as possible, S_u is required to be close to zero in the low frequency range to improve the disturbance suppression ability. T_u is as close to zero as possible in the high frequency range to improve the system noise suppression ability. Therefore, the desired loop function $L = G_u(s)K(s)$ satisfies that it has a low gain in the low frequency range and a high gain in the high frequency range. First, the spectrum of $W(s)$ is analyzed. Figure 2 shows the singular value curve of the external disturbance $W(s)$, also known as the singular value curve of the open-loop transfer function.

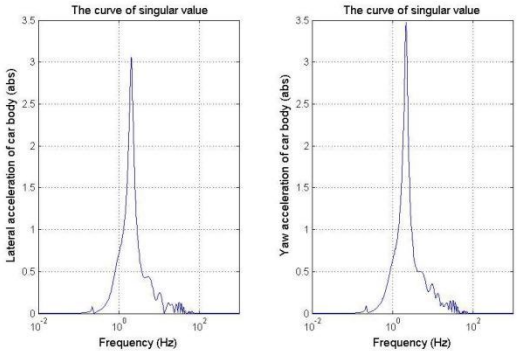

Figure 2: The singular value curve of the external disturbance $W(s)$.

It can be seen from Figure 2 that the external disturbance $W(s)$ has a dominant natural frequency $w_n = 2.18Hz$. When the frequency is less than $0.5Hz$ and higher than $50Hz$, the singular value (absolute value) of external disturbance $W(s)$ is close to zero. Based on the equation (14),we can get that in the range of $0.5Hz \sim 50Hz$, the value of the sensitivity function S_u no longer determines the output $Y(s)$. Therefore, as long as the designed controller can restrain the external disturbance within the range of $0.5Hz \sim 50Hz$, it can have good control effect. Of course, in order to obtain better control effect, the controller designed should have a wider frequency disturbance suppression range.

Figure 3 shows the singular value curve of the train system G_u. As can be seen from the figure, when the frequency is lower than $0.01Hz$, the system has a very low singular value. No matter how the controller is selected, the loop transfer function and sensitivity function satisfies $L = G_u K \approx 0$ and $S_u \approx 1$, respectively. The S_u is no longer the decisive factor determining the system output.

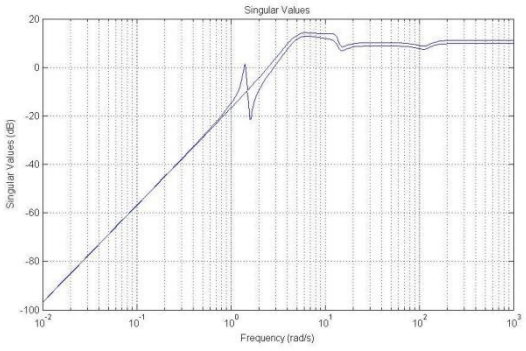

Figure 3: Singular value graph of the train system G_u.

In summary, the frequency below $0.5Hz$ can be ignored in the design of vibration reduction for train system. Therefore, the following work in this paper is to shape the open-loop system by setting the preposition and post-position weight matrix function at frequencies above $0.5Hz$, so that the loop function is close to the desired function.

Due to $S + T = 1$, the sensitivity performance index satisfies $\|W_1 S\|_\infty < 1$, and the complementary sensitivity performance index satisfies $\|W_2 T\|_\infty < 1$, and there is a relationship between them: $\|W_1 S| + |W_2 T\|_\infty < 1$. As we can known, the performance design goal and the robust stability goal are a pair

ISSN 2616-5767 Vol.8, Issue 3: 41-50, DOI: 10.25236/AJETS.2025.080307

of contradictory and mutually constrained control goals. Therefore, it is very important to choose the appropriate weight matrix function to achieve a compromise between the control performance and the robust stability of the system. When solving the robust stabilization controller, the selection of the weight matrix function should meet the following requirements:

$$\begin{aligned}\left|W_1^{-1}(s)\right| &\geq \bar{\sigma}\left[S(jw)\right] \\ \left|W_2^{-1}(s)\right| &\geq \bar{\sigma}\left[T(jw)\right]\end{aligned} \tag{15}$$

Where $W_1^{-1}(s)$ has high pass characteristics; $W_2^{-1}(s)$ has low pass characteristics.The maximum peak M_S of the sensitivity function satisfies the equation $M_S = \max_w \left|S(jw)\right| = \left\|S\right\|_\infty$; The maximum peak M_T of the complementary sensitivity function satisfies the equation $M_T = \max_w \left|T(jw)\right| = \left\|T\right\|_\infty$. In order to avoid poor system performance and robust stability, the values of M_S and M_T should not be too large (higher than 4). In general, there are the following requirements for the peak value: $M_S < 2, M_T < 1.25$.

In order to achieve low frequency and high gain, the diagonal elements of the pre-compensation matrix function are usually in the form of proportional integral (PI): $w_1(s) = \left(s/M + w_b\right)/\left(s + w_b * A\right)$. Where M is the gain attenuation coefficient at high frequency. Usually selected as M=2;. A is the gain at low frequency; w_b is the minimum bandwidth frequency. M, A and w_b are used as knobs to adjust the sensitivity function. They determine the minimum bandwidth and amplitude of the sensitivity function at low and high frequencies respectively.

The purpose of post-compensator W_2 is to achieve noise suppression, so W_2 should include a low-pass filter for hysteresis correction to achieve low gain in high frequency range. In general, the desired low gain requirement can also be obtained by introducing an integral part. Finally, for the diagonal form of weight matrix, designers can directly adjust the weight between each input and output channel by experience and accumulation, so as to realize the adjustment of output results.

After the above analysis, the diagonal elements of the weight function W_1 for the train system are selected as follows: $w_1(s) = \left(2.5s + 100\right)/\left(s + 0.1\right)$ .The weight matrix function W_1 is presented as: $W_1(s) = \begin{bmatrix} w_1(s) & 0 \\ 0 & w_1(s) \end{bmatrix}$. The diagonal elements of the weight function W_2 are selected as: $w_2(s) = w_\partial(s) * \left[1/\left(0.005s + 1\right)\right]$. Where $w_\partial(s) = \left(0.002s + 1\right)/\left(0.03s + 1\right)$. The final weight function W_2 is denoted as: $W_2(s) = \begin{bmatrix} w_2(s) & 0 \\ 0 & w_2(s) \end{bmatrix}$. Thus, the desired loop transfer function can be expressed as:

$$\begin{aligned}\left|W_1^{-1}(s)\right| &\geq \bar{\sigma}\left[S(jw)\right] \\ \left|W_2^{-1}(s)\right| &\geq \bar{\sigma}\left[T(jw)\right]\end{aligned} \tag{16}$$

The comparison of singular value curves between the train system before shaping and the desired train system is shown in Figure 4.

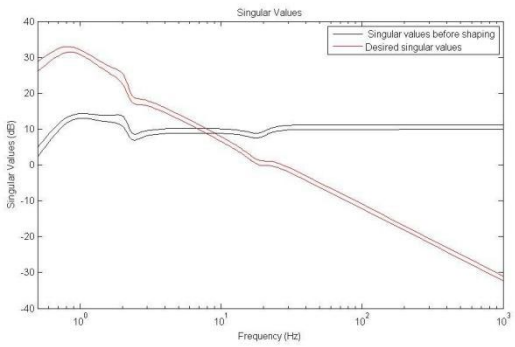

Figure 4: Comparison diagram of singular value curve before shaping and desired.

It can be seen from Figure 4 that the shape of the desired singular value curve of the train system meets the design requirements: the low frequency band has high gain,and the high frequency band has

ISSN 2616-5767 Vol.8, Issue 3: 41-50, DOI: 10.25236/AJETS.2025.080307

low gain. Hence, we can get the selected weighting function can make the system have good performance robustness.

3.2 Robust stabilization for normalized coprime factor perturbations

Consider the desired loop transfer function of the train system :

$$G_s(s)=\begin{bmatrix} A_s & B_s \\ C_s & D_s \end{bmatrix}=\begin{bmatrix} w_2Aw_1 & w_2B_2w_1 \\ w_2C_1w_1 & w_2D_2w_1 \end{bmatrix} \tag{17}$$

Solving the robust stabilization controller $K\infty$ for a normalized corprime factor perturbed plant:

$$\inf_k \left\| \begin{bmatrix} K_\infty \\ I \end{bmatrix} (I+G_SK_\infty)^{-1}\tilde{M}_S^{-1} \right\|_\infty = (1-\left\| \begin{bmatrix} \tilde{N} & \tilde{M} \end{bmatrix} \right\|_H^2)^{-1/2} = \frac{1}{\sqrt{1-\lambda_{\max}(XZ)}} = \gamma_{\min} = \varepsilon_{\max}^{-1} \tag{18}$$

Where $\|\bullet\|_H$ is *Hankel* norm; $\lambda_{\max}$ is maximum eigenvalue.We can get that the maximum stability margin of the train system can be expressed as:

$$\varepsilon_{\max}=(1-\left\| \begin{bmatrix} \tilde{N} & \tilde{M} \end{bmatrix} \right\|_H^2)^{1/2}=\sqrt{1+\lambda_{\max}(XZ)}<1 \tag{19}$$

X and Z are the unique positive definite solutions to the Riccati algebraic equations expressed in Equation (20):

$$\begin{cases} (A_S-B_SS^{-1}D_S^*C_S)X+X(A_S-B_SS^{-1}D_S^*C_S)-XB_SS^{-1}B_S^*X+C_S^*(I-D_SS^{-1}D_S^*)C_S=0 \\ (A_S-B_SD_S^*R^{-1}C_S)Z+Z(A_S-B_SD_S^*R^{-1}C_S)-ZC_S^*R^{-1}C_SZ+B_S(I-D_S^*R^{-1}D_S)B_S^*=0 \end{cases} \tag{20}$$

Where $S=I+D_S^*D_S$, $R=I+D_SD_S^*$.

By calculating formula (19) and (20) in MATLAB, we can get the maximum robust stability boundary of the train system $\varepsilon_{\max}=0.5512$.

In order to meet the robust stability requirements of the train system, the performance index can also be further improved. Therefore,letting $\varepsilon=0.3<\varepsilon_{\max}$, there exists:

$$\inf_k \left\| \begin{bmatrix} K_\infty \\ I \end{bmatrix} (I+G_SK_\infty)^{-1}\tilde{M}_S^{-1} \right\|_\infty < \varepsilon^{-1} \tag{21}$$

By solving equation (21), $H\infty$ loop shaping robust stabilization controller with stability margin $\varepsilon=0.3$ can be obtained:

$$K_\infty=\begin{bmatrix} A_S+B_SP+\varepsilon^{-2}(Q^T)^{-1}ZC_S^T(C_S+D_SP) & \varepsilon^{-2}(Q^T)^{-1}ZC_S^T \\ B_S^TX & -D_S^T \end{bmatrix} \tag{22}$$

Where $P=-S^{-1}(D_S^TC_S+B_S^TX)$, $Q=(1-\varepsilon^{-2})I+XZ$.

By combining with the weights functions W_1 and W_2, the final 2-input-2-output $H\infty$ loop shaping controller is obtained:

$$K=W_1K_\infty W_2 \tag{23}$$

3.3 Controller model reduction

Due to the order of $H\infty$ loop shaping controller of train system is 46. Hence, the Hankel norm optimal algorithm is used to reduce the order of the controller model. This model reduction method was first proposed by British scholar Glover.

Hankel singular values $\sigma_i(i=1,2,.....,46)$ of the $H\infty$ loop shaping controller are:333.3738, 325.6090, 53.6655, 50.2857, 5.9009, 5.5730, 1.694 0, 1.6629, 0.1600, 0.1493, 0.1093, 0.0875, 0.0667, 0.0601, 0.0360, 0.0345, 0.0240, 0.0219, 0.0135, 0.0134, 0.0014, 0.0011, 0.0003, 0.0002, 0, 0,0, 0, 0, 0, 0, 0, 0, 0, 0, 0, 0, 0, 0, 0, 0, 0, 0, 0, 0, 0, 0, 0, 0. The eighth singular value and the ninth singular value have relatively large numerical jump. Moreover, the values from the 9th to the 46th are all small, indicating that the relative energy of the controller in these order states is small and has little influence on the system.

ISSN 2616-5767 Vol.8, Issue 3: 41-50, DOI: 10.25236/AJETS.2025.080307

Thus, consider computing the eighth-order approximation of the controller $K(s)$, and let it be $Kr(s)$. The Hankel singular value curve of the controller is shown in Figure 5.

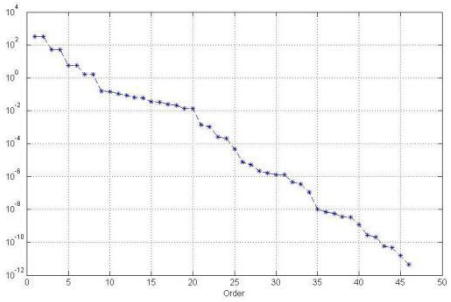

Figure 5: The Hankel singular value curve of $H\infty$ loop shaping controller.

The coefficient matries of the state space equation of the final controller after order reduction are expressed as follows:

$$A_{Kr}=\begin{bmatrix} -0.0762 & -0.0018 & 0.0017 & 0.0354 & 0.0162 & -0.0140 & -0.0069 & 0.0075 \\ 0.0019 & -0.0779 & -0.0366 & 0.0020 & 0.0039 & -0.0034 & 0.0074 & 0.0067 \\ -0.0057 & 0.0361 & -0.0183 & 0.0025 & 0.0040 & -0.0037 & 0.0095 & 0.0080 \\ -0.0350 & -0.0059 & -0.0023 & -0.0198 & -0.0187 & 0.0213 & 0.0090 & -0.0106 \\ -0.0162 & -0.0038 & 0.0005 & -0.0192 & -0.0492 & 1.5949 & 0.0429 & -0.0747 \\ -0.0141 & -0.0032 & 0.0011 & -0.0216 & -1.5949 & -0.0422 & -0.0221 & 0.0395 \\ -0.0069 & 0.0074 & -0.0106 & -0.0075 & -0.0431 & -0.0229 & -0.0652 & 0.0018 \\ 0.0075 & 0.0068 & -0.0066 & 0.0117 & 0.0746 & 0.0390 & 0.0033 & -0.0665 \end{bmatrix} \quad B_{Kr}=\begin{bmatrix} -6.0387 & -3.7861 \\ 3.7882 & -6.0289 \\ -0.9455 & 1.0325 \\ -1.0405 & -0.9541 \\ -0.5375 & -0.5407 \\ -0.4863 & -0.4836 \\ -0.4553 & 0.1164 \\ 0.1342 & 0.4508 \end{bmatrix}$$

$$C_{Kr}=\begin{bmatrix} -6.0555 & 3.7579 & 0.7697 & 1.1724 & 0.5389 & -0.4845 & -0.4544 & 0.1375 \\ -3.7591 & -6.0479 & -1.1695 & 0.7865 & 0.5393 & -0.4855 & 0.1198 & 0.4498 \end{bmatrix} \quad D_{Kr}=\begin{bmatrix} 0 & 0 \\ 0 & 0 \end{bmatrix}$$

The sensitivity function and the complementary sensitivity function constituted by $Kr(s)$ can be denoted as $S_u=1/(1+G_uKr)$ and $T_u=G_uKr/(1+G_uKr)$. The maximum peaks M_S and M_T of S_u and T_u can be calculated as:

$$M_S=1.3058;\ M_T=1.0224 \tag{24}$$

Satisfy the requirements.

Figure 6 shows the singular value curve of the sensitivity function S_u. It can be seen from the figure that: in the low frequency , S_u has a small singular value, which reflects that the designed controller can make the train system achieve good disturbance suppression effect. In the high frequency range, the singular value is close to unit. Based on the relation that the sum of S_u and T_u is equal to unit, it can be known that the complementary sensitivity function has a small singular value at high frequencies, which reflects that the designed controller can achieve good noise suppression effect for the train system.

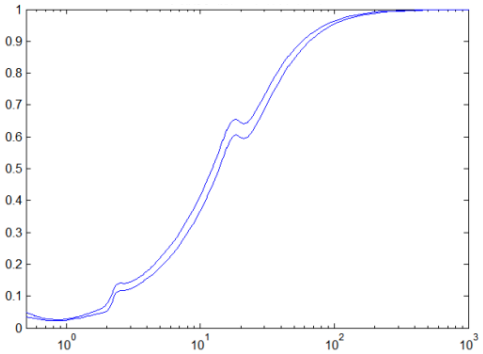

Figure 6: The singular value curve of the sensitivity function S_u.

ISSN 2616-5767 Vol.8, Issue 3: 41-50, DOI: 10.25236/AJETS.2025.080307

4. Conclusions Simulation validation and evaluation

In order to show the efficiency of the proposed $H\infty$ loop shaping controller, the multi-body dynamics simulation model of CRH3 is built in SIMPACK, as shown in Figure 7.

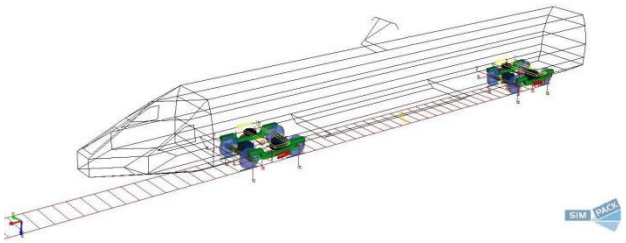

Figure 7: Multi-body dynamic model of CRH3.

Letting the simulation running speed as 300km/h and the simulation running time as 100s. Considering the German low disturbance track irregularities and German high disturbance track irregularities, the vibration profiles of open loop and $H\infty$ loop shaping control are shown in Figure. 8. The mean squares and peaks are given in Table 3. The operation stability index are listed in Table 4. According to the table, after using the loop shaping control strategy, the operation stability is improved by about 33% and 31% compared with the open loop for low and high disturbance respectively.

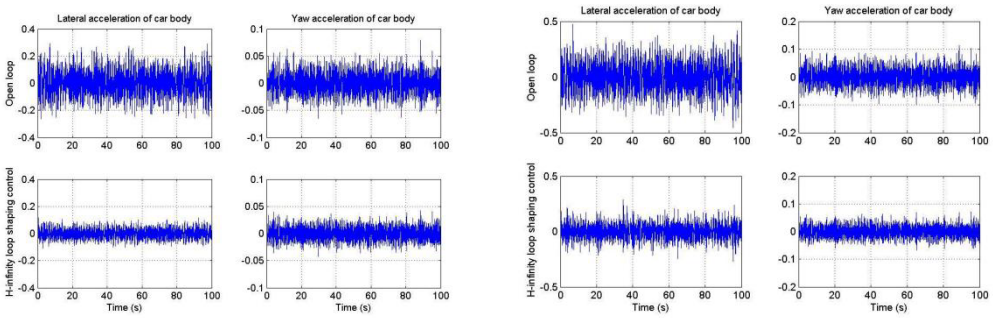

Figure 8: Vibration profiles for German disturbance track irregularities.

Table 3: The mean squares and peaks for track irregularities.

		lateral acceleration		YAW ACCELERATION	
		Mean squares	Peaks	Mean squares	Peaks
low disturbance	Open loop	0.0851	0.2928	0.0187	0.0785
track irregularities	Controller	0.0308	0.1153	0.0109	0.0424
high disturbance	Open loop	0.1179	0.4743	0.0292	0.1128
track irregularities	Controller	0.0568	0.2866	0.0181	0.0704

Table 4: The operation stability index for track irregularities.

		Operation stability index
low disturbance	Open loop	2.4173
track irregularities	Controller	1.6165
high disturbance	Open loop	2.8153
track irregularities	Controller	1.9425

5. Conclusions

The purpose of this paper is to suppress the lateral vibration of train body and improve the operation stability. To suppress both external disturbance and noise for high-speed train, the $H\infty$ loop shaping control method was proposed to the lateral active/semi-active suspension system. In order to realize the robust stability requirement at the same time, the stability margin is set as 0.3. Based on the fact that the designed controller is a high-order model, a Hankel norm optimal algorithm is used to reduce the order. And then the full-scale train model of CRH3 was established in SIMPACK to test the effectiveness of loop shaping control method. The simulation results of German low and high disturbance track irregularities show that the $H\infty$ loop shaping control can successfully suppress the vibration of high-

ISSN 2616-5767 Vol.8, Issue 3: 41-50, DOI: 10.25236/AJETS.2025.080307

speed railway and improve operation stability.

References

[1] Thompson A G. Design of active suspensions. Proceedings of the Institution of Mechanical Engineers, 1970, 185(1):553-563.
[2] Goodall R. Active railway suspensions: Implementation status and technological trends. Vehicle System Dynamics, 1997, 28(2-3):87-117.
[3] Goodall R M, Kortum W. Active controls in ground transportation-A review of the stare-of-the-art and future potential. Vehicle System Dynamics, 1983,12(4-5):225-257.
[4] Crosby M J, Karnopp D C. The active damper: a new concept for sock and vibration control. Shock and Vibration Bulletin, 1973,43(4).
[5] Karnopp, D. Design Principles for Vibration Control Systems Using Semi-Active Dampers. ASME Journal of Dynamic Systems, Measurement, and Control, 1990,112(3):448-455.
[6] L. Jezequel, V. Roberti, B.Ouyahia, and Y. Toutain, Improvement of very high speed trains comfort with preview semi-active suspensions, Vehicle System.Dynamics. 1992, 20(S1):299-313.
[7] Peel D J , Stanway R , Bullough W A . Dynamic modelling of an ER vibration damper for vehicle suspension applications[J]. Smart Materials & Structures, 1996, 5(5):591.
[8] Liao W H , Wang D H . Semiactive Vibration Control of Train Suspension Systems via Magnetorheological Dampers[J]. Journal of Intelligent Material Systems & Structures, 2003, 14(3):161-172.
[9] Lau Y K , Liao W H . Design and analysis of a magnetorheological damper for train suspension[C]// Smart Structures and Materials 2004 Conference. 2004.
[10] Fotoohi A , Yousefikoma A . Active control of train bogies with MR dampers[C]// Smart Structures & Materials. International Society for Optics and Photonics, 2006.
[11] Guo, Jin, Xu, et al. A new semi-active safety control strategy for high-speed railway vehicles[J]. Vehicle System Dynamics: International Journal of Vehicle Mechanics and Mobility, 2015.
[12] Wang, D. H. , and W. H. Liao . "Semi-active suspension systems for railway vehicles using magnetorheological dampers. Part I: system integration and modelling." Vehicle System Dynamics.
[13] Wang, D. H. , and W. H. Liao . "Semi-active suspension systems for railway vehicles using magnetorheological dampers. Part II: simulation and analysis." Vehicle System.
[14] Qiao Z , Ding J J , Yang M L . LQG Control Based Lateral Active Secondary and Primary Suspensions of High-Speed Train for Ride Quality and Hunting Stability[J]. IET Control Theory & Applications, 2018, 12:1497-1504.
[15] Yu J S , You W H , Hur H M , et al. H∞ Control of Secondary Suspension in Railway Vehicles Equipped with a MR Damper[J]. Journal of the Korean Society for Precision Engineering, 2013, 30(10).
[16] Guo C , Gong X , Xuan S , et al. Semi-active H infinity control of high-speed railway vehicle suspension with magnetorheological dampers. 2013.
[17]Song, Yong Duan , and X. Yuan . "Low-cost Adaptive Fault-tolerant Approach for Semi-active Suspension Control of High Speed Trains."IEEE Transactions on Industrial Electronics(2016):1-1.
[18] Metin M , Guclu R . Active vibration control with comparative algorithms of half rail vehicle model under various track irregularities[J]. Journal of Vibration & Control, 2011, 17(10):1525-1539.
[19] Li G , Jin W , Chen C . Fuzzy Control Strategy for Train Lateral Semi-active Suspension Based on Particle Swarm Optimization[J]. Springer, Berlin, Heidelberg, 2012.
[20] Mcfarlane, D , K. Glover , and M. Noton . "Robust stabilization of a flexible space platform: an H∞, coprime factor approach." International Conference on Control IET, 1988.
[21] Civita, M. La , et al. "Design and Flight Testing of an H00 Controller for a Robotic Helicopter." Journal of Guidance, Control, and Dynamics 29.2(2006):485-494.
[22] Buerger, S. P. , and N. Hogan . "Complementary Stability and Loop Shaping for Improved Human–Robot Interaction."IEEE Transactions on Robotics 23.2(2007):232-244.
[23] Park, Kyihwan , et al. "An Active Vibration Isolation System Using a Loop Shaping Control Technique." IEEE/ASME International Conference on Mechtronic & Embedded Systems & Applications IEEE, 2008.